TESTS ON ROUGING AND EXPERIENCES DEALING WITH ROUGING IN PHARMACEUTICAL PRODUCTION

Thomas Blitz, Ernst Felber, Robert Haas, Birgit Lorsbach, Andreas Marjoram, Roland Merkofer, Tobias Mueller, Nathalie Schuleit, Marc Vernier and Thomas Wellauer

Part 2 of this article describes tests and practical experiences in rouging formation and the influence of rouge coatings on cleaning efficiency.

Abstract

The present technical article (in 3 parts) discusses the current body of knowledge on the subject of rouging. It is based on insights from tests and operating experiences of companies that manufacture pharmaceutical medicinal products.

By means of a generic risk-based approach and a test setup derived from this, it is shown that the danger resulting from rouging for products and patients may be regarded as slight. As regards products, however, a conclusive appraisal may be obtained only by means of specific risk analyses. The risks resulting from derouging actions must also be considered in the overall assessment.

Part 1 of this article described the background on rouging, rouging formation, derouging and a risk overview.

Tests and Practical Experiences

The procedure for corrosion investigations is described in DIN 50905 Parts 1-5. The most important principles for conducting material compatibility tests are explained here.

During the investigations, the conditions for the various investigation parameters must be accurately defined and complied with. First it must be ensured that the correct material with the desired surface quality is available. Then the test conditions such as temperature, pressure and composition of the test medium must be defined and a suitable test apparatus selected.

During the course of the test, which usually lasts at least 4 weeks, it must be ensured that the parameters do not stray above or below the values fixed for them. An appropriate instrumentation and control system is required for this purpose. After the tests, an exact gravimetric and optical evaluation of the samples is usually made. For this purpose, a suitable analytical balance and a microscope must be available.

The limit value for technical resistance corresponds to a material removal rate of < 0.1 mm/a (millimeters per year). The requirements for pharmaceuticals or food products may be more stringent, however, since product contamination by heavy metals must also be prevented in these cases. The difficulty of the rouging investigation is that, even after long test periods (several months), it has usually been impossible to simulate the surface changes in the laboratory test. Furthermore, no significant material removal rates were measurable.

Occurrence of Rouging Under the Effect of Clean Steam

To investigate rouge formation in clean steam systems, electropolished test plates of materials 1.4435, 1.4539 and 1.4571 were introduced into a clean steam system (138°C, 2.5 bar gauge). The weight variation was recorded as a function of time in order to determine a material-specific corrosion rate.

After an uninterrupted exposure time of 824 days, the test plates exhibited non-uniformly formed black, partly brownish discolorations (Figure 1). These discolorations exhibited only slight similarities to the rouge coatings observed on media-contacted surfaces of clean steam systems after prolonged operating times.

Because of the very small and unsteady weight changes of the test plates, it was not possible to determine the corrosion rates. Instead, the variation of the weight change over the test time was reported (Figure 2). A comparatively high corrosion rate of 3.4×10^{-3} mm/a, as has been determined for WFI systems (at 85°C),[9] could not be confirmed for the investigated materials in a clean steam system.

Figure 1 Test plates after an exposure time of 824 days

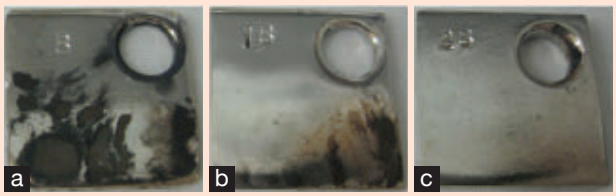

(a) material 1.4571 (b) material 1.4435 (c) material 1.4539

Figure 2 Graph of the weight change of the test plates exposed to clean steam

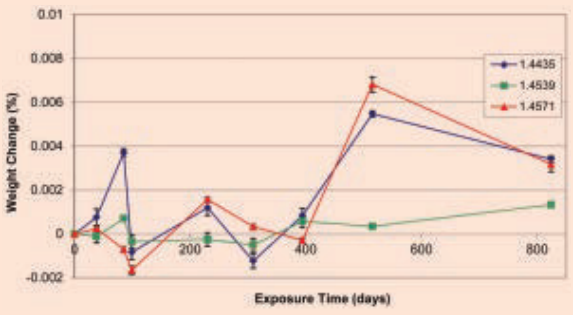

Influence of Hot Sodium Hydroxide Solution on Stainless Steel Surfaces

The materials 1.4404, 1.4435, 1.4539, 1.4591, 2.4600 and 2.4602 were investigated as regards their behavior toward hot sodium hydroxide solution.

Electropolished test plates of the materials were exposed continuously to sodium hydroxide solution (1% NaOH; temperature ≥ 78°C). The material-specific corrosion rates were determined by weighing the test plates at regular intervals to measure their change in weight. Moreover, the surface conditions were visually appraised and the surface topographies and compositions were analyzed by means of SEM and ESCA.

With the exception of material 1.4591, all test plates exhibited a different, material-dependent weight loss. Furthermore, distinct discolorations of the surfaces were observed for all test plates. Both these weight losses and color changes depended directly on the exposure time of the test plates. They are greatest for materials 1.4404 and 1.4435, whereas materials 1.4539, 1.4591, 2.4600 and 2.4602 exhibited much smaller weight differences as shown in Figure 3.

It was possible to calculate material-specific corrosion rates from the weight losses (Figure 4). A positive value corresponds here to a decrease of material thickness, while a negative value indicates an increase, as is possible, for example, due to formation of an oxide/hydroxide layer.

On the basis of material analyses (ESCA), the discolorations of the test plates can be attributed to a layer formed in the course of the test from chromium(III) oxide (Cr_2O_3) or chromium(III) hydroxide ($Cr(OH)_3$ or respectively from nickel(III) oxide (Ni_2O_3) or nickel(III) hydroxide (Ni_2O_3*H_2O). (ESCA is unable to distinguish between oxides and hydroxides.) Compared with the matrix, material 1.4435 exhibited distinct changes down to depths of 200 to 250 nm, whereas for 1.4539 this is the case down to depths of only approximately 100 nm. For the investigated materials 1.4404, 1.4435 and 1.4539, the alloying element iron was almost completely absent in the near-surface layers (approximately 50 to 150 nm) (Figure 5).

The thickness of the oxide or hydroxide layer was determined from the half-height of the oxygen curve (red broken line in the ESCA profiles of the exposed test plates) and is presented in Table A. A possible explanation for the presence of magnesium down to sputter depths of 150 to 200 nm is the recycling of sodium hydroxide solution in this type of CIP plant. So magnesium contained in trace element solutions as used in biotechnological

Figure 3 Weight variation of the test plates exposed to sodium hydroxide solution

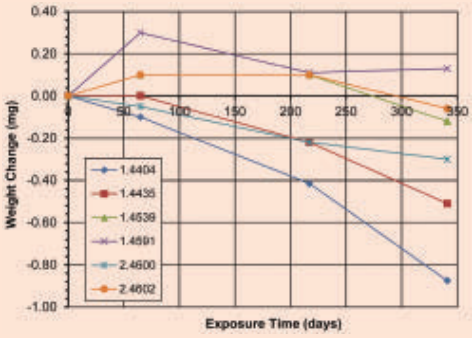

Figure 4 Material-specific corrosion rates for the maximum exposure time of 354 days

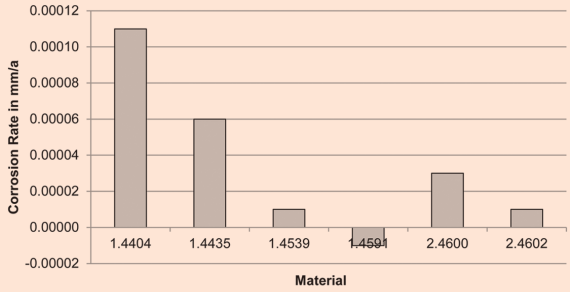

fermentation processes could get into the sodium hydroxide CIP solution during cleaning of process equipment and finally enriched in the oxide/hydroxide layers of the exposed samples.

The SEM photographs revealed porous crystalline surface structures for material 1.4435, while material 1.4539 exhibits this to a much smaller extent (Figure 6).

The oxide layers formed during exposure to alkaline solution were bonded very stably with the surface and could not be removed by wiping. Thus release of particles into neighboring medium is not expected from such altered surfaces during the investigated exposure period. Nevertheless, the leaching of iron from the surface layers of the materials favors rouge formation in other system components. It may well be that the presence of atmospheric oxygen leads to oxidation of the iron hydroxide dissolved in the alkaline solution to sparingly soluble iron oxides, which are able to settle as migration rouge on system components.

Table A Half height of the oxygen curve of the material samples for the maximum exposure time of 354 days

Material	Relative Sputter Depth (nm)	
	Exposed	Reference
1.4404	240	≤ 5
1.4435	40	≤ 5
1.4539	85	≤ 5

Figure 5 ESCA depth profile

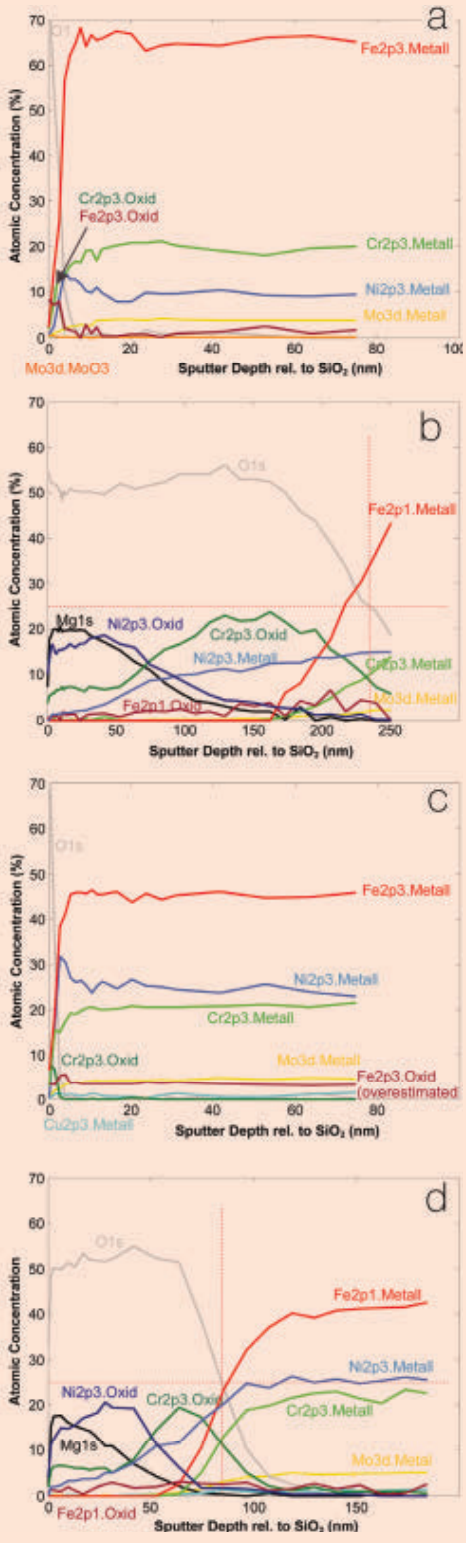

(a) reference material sample 1.4435, (b) material sample 1.4435 after exposure to NaOH, (c) reference material sample 1.4539 and (d) material sample 1.4539 after exposure to NaOH

Figure 6

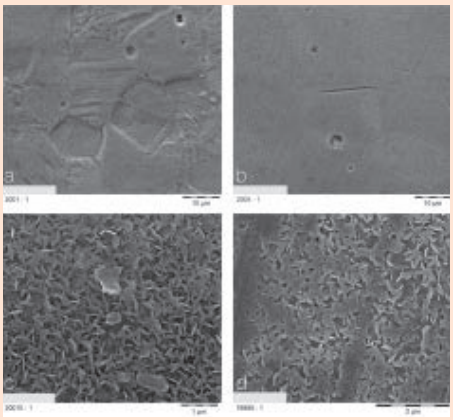

(a) reference material sample 1.4435 [SEM photograph with a magnification of 2001:1; topography contrast (SE), 5 kV], (b) reference material sample 1.4539 [SEM photograph with a magnification of 2001:1; topography contrast (SE), 5 kV], (c) material sample 1.4435 after exposure to NaOH [SEM photograph with a magnification of 20,010:1; topography contrast (SE), 5 kV] and (d) material sample 1.4539 after exposure to NaOH [SEM photograph with a magnification of 19,890:1; topography contrast (SE), 5 kV]

Figure 7 Test plates of 1.4435

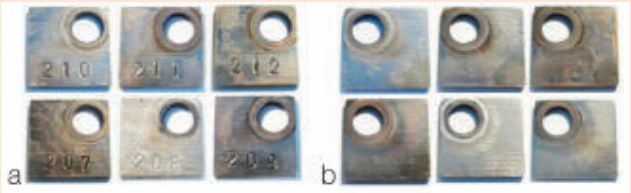

(a) front side and (b) back side – arrangement analogous to (a).
Note: 210, 211, 212 is upper zone of tank; 207, 208, 209 is lower zone of tank. 208 and 210 were subjected to derouging

Rouge Formation due to Alternating Stress on Materials by Cleaning and Sanitizing Processes

To investigate the influence of the combination of cleaning and sanitizing processes on rouge formation, material-specific corrosion rates of various materials caused by exposure to various cleaning and sanitizing media were to be measured.

Electropolished test plates of materials 1.4404, 1.4435 and 1.4539 were subjected to combined cleaning/sanitizing cycles (10 minutes of rinsing with 1% sodium hydroxide solution; temperature ≥ 78°C; 30 minutes of sanitizing with clean steam: temperature > 121°C, 2.5 bar gauge). During cleaning with sodium hydroxide solution, one part of the test plates was above the liquid level, while the other part was immersed in the solution.

Figure 8 Weight variation of the test plates exposed to CIP/SIP

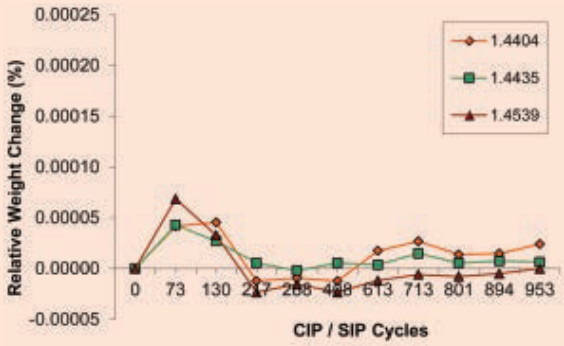

At the end of the test, all test plates exhibited reddish-brown discolorations typical of rouging on the surface, darker in the test plates that had been immersed in sodium hydroxide solution. Test plates 208 and 210, which had a distinctly paler appearance, were subjected after half of the test period to acid-based derouging, in order to check the resistance of these materials to an acid derouging chemical (Figure 7). After completion of derouging, these test plates were further exposed to the cleaning/sanitizing cycles.

A significant change in weight of the test plates due to rouge formation could not be observed. Because of the very small and non-uniform weight changes, it was not possible to determine material-specific corrosion rates. At this juncture, therefore, a graph of the relative weight change versus experiment time was chosen (Figure 8). The supposed weight increase at the beginning of the test (73 and 130 CIP/SIP cycles respectively) was attributed to inadequate rinsing of the test plates, such that residues of the sodium hydroxide solution were not completely removed.

It is highly likely that the slight weight increase in the further course of the test (from cycle 217 on) can be explained by the adsorption of oxygen in the oxide-rich rouge layer being built up in conjunction with the lack of material removal from this layer.

Table B Components and the respective investigations carried out on them

Object	Optical Finding	SEM Investigation	ESCA Analysis	AES Analysis
Spray ball in a PW storage tank	x		x	x
Filter of a WFI system	x	x	x	
Wipe sample from the surface of a WFI system	x	x		

Figure 9 Spray ball in a PW storage tank

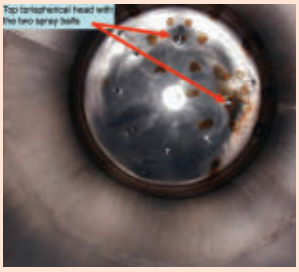

Figure 10 Dismantled spray ball from a PW storage tank

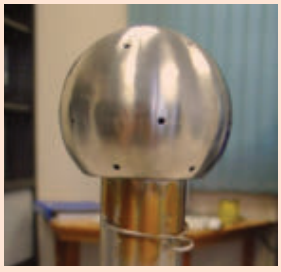

Figure 11 Depth profile by ESCA of the reddish inner surface of the spray ball

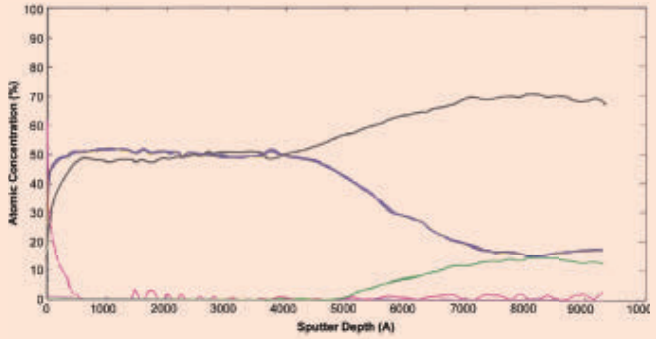

Figure 12 Filter of WFI system with discolored bluish inside surface

Investigations by Surface Analysis and Determination of the Corrosion Rate of Components from Purified Water Systems

Investigations were carried out on rouged components from various WFI systems in order to obtain more information about the actual buildup of rouge layers, which are formed in such systems. The investigations carried out on the respective components are presented in Table B and respective stress conditions listed in Table C. The detailed results for the individual components are presented below.

Spray Ball of a PW Storage Tank

The tank exhibits local surface discolorations, in particular precisely where the sprayed water impacts the tank surface (Figure 9). The spray ball itself exhibits yellowish to slightly reddish discolorations only on the supply tube (Figure 10). The inside surface exhibits an intense reddish coating. This was further investigated by surface-analysis techniques. In particular, depth profiles were surveyed by means of Auger electron spectroscopy (AES) and ESCA, in order to determine the variation of the alloying elements over the depth (Figure 11).

The samples were degreased and sputtered before the spectroscopic investigations, in order to remove potential carbon-containing impurities that may have been introduced by handling after dismantling. In both cases, it was found that the layer is approximately 600 nm thick and consists predominantly of iron and oxygen. This iron is present as FeO and FeO(OH). The other alloying elements – chromium, nickel and molybdenum – were not found.

Filter from a WFI System

A comparable result was found on a filter from a WFI system. The filter had been in service for approximately 6 months at 80°C, in a flow arriving from the inside. The outside surface has a slightly brownish appearance, while the discoloration of the inside surface is predominantly bluish (Figure 12). Only the attachment zone and the tip are metallically bright. The SEM investigation undertaken revealed that the bluish surface is formed from a closed layer consisting of many fine crystals. The average crystal size is approximately 0.2 µm. In contrast, only individual particles with a size of 0.1 µm can be observed in the metallically blank zone (Figure 13).

The depth profile recorded by means of ESCA (Figure 14) shows the variation of the alloying elements down to a depth of approximately 100 nm. The high carbon and silicon contents directly at the surface can be attributed to the adsorption of CO_2 and silicone compounds, which among other possibilities presumably reached the surface during handling after service. Because the surface is highly structured, these impurities can be measured to even greater depths. The layer is more than 120 nm thick, since oxygen contents of > 25% were still determined down to this zone and significant contents of carbon and silicon are also still present. In the first 60 nm, the chromium content is very low, while nickel and molybdenum are virtually absent.

Iron and chromium are present directly at the surface as Fe^{3+} and Cr^{3+} respectively.

Condition of a WFI System

A WFI system was optically appraised by opening the system at several places and investigating the coatings there by means of SEM and EDX. The results for the rouged zones are summarized in Table F.

The coatings were picked up from the surface by means of a cloth and then analyzed by means of SEM. The coatings contained predominantly oxygen, iron and chromium. Samples that were presumably rubbed more vigorously also exhibited nickel and a relatively low oxygen content (Figure 15).

Summary
The surface of metallic materials such as 316L is altered during rouge formation. The passive layer, which is a few nm thick and has a high chromium content, is changed to an iron-rich layer that also has relatively low contents of chromium and nickel. Depending on time and nature of the exposure, the layer thickness grows to more than 600 nm. The surface texture is changed from metallically smooth to a crystalline structure.

In order to simulate the rouging process and to investigate it further as regards the buildup of the rouge layer and the corrosion rate, electropolished seamless base-metal samples of various austenitic standard materials were aged in a WFI distillation system showing signs of rouging. The exposure time was 21 days at 108°C. The results of the optical examination and of the gravimetric evaluation are summarized in Table G.

When the samples were removed, they exhibited a metallically bright surface and no signs of rouging. The measured rates of material removal ranged from $4*10^{-4}$ to $18*10^{-4}$ mm/a.

Heavy Metal Concentrations in Purified Water Systems and Active Substance Solutions
During monitoring of PW/WFI systems, it is common practice to determine, among other parameters, the heavy metal ion concentration in the water. According to the European Pharmacopoeia 6.2 (2008), a total limit value of < 100 ppm is defined for this. The limit values according to the EMEA Guideline for active substance solutions are differentiated according to the individual metal species and are much lower for the elements other than iron and zinc. They are therefore used as reference. The results of water analysis from various circuits are summarized in Table H. ICP MS was used for the determination.

The results show that, in a normally operated water circuit in which fresh water is regularly injected and removed, no measurable enrichment of heavy metal ions takes place and their concentrations are below the limit values of the EMEA Guideline by a factor of 10.

Under non-typical operating conditions, in which the water is merely circulated in the circuit for weeks, for example to prevent a hygiene risk to the system during a production shutdown, an increase of the nickel content due to enrichment may occur. In such exceptions, it should be checked, for example by analyses, whether a limit value violation exists and whether the water purity may have to be adjusted safely below the limit values by partial or complete replacement of the water.

Furthermore, it was investigated whether active substance solutions produced in production systems made of structural

Table C	Stress conditions of the investigated components				
Water Quality	Temperature	Hot Steps	Material	Appearance	Age
PW	40°C	85°C once per year (5 h)	1.4571 1.4404	▸ Tank localized points ▸ Spray ball inside complete reddish	n/a
WFI	80	None	1.4571 1.4404	Outside: brownish Inside: bluish	6 months
WFI	> 80°C	None	1.4571 1.4404	See Table I	24 years

materials 1.4435 exhibit elevated heavy metal concentrations. For this purpose, the heavy metal concentration of active substance solutions from various systems of different age was investigated.

Table I shows the systems in question with the year when they were placed in service and the respective active substance solution produced in the system. At the end of the production process, samples of three successive batches of the respective active substance were investigated by means of ICP MS to determine their heavy metal concentration.

For all investigated API samples, the results of the heavy-metal analysis were below the limit of quantitation of the analysis method and therefore well below the requirements of the EMEA[12], regardless of the degree of rouging and of any derouging actions that may have been performed.

Influence of Rouge Coatings on Cleaning Efficiency

The cleanability of rouged material surfaces was investigated.

Rouging was caused in a test tank by a rapid sequence of combined cleaning/sanitizing cycles (10 minutes of cleaning with 1% sodium hydroxide solution, temperature ≥ 78°C, then 30 minutes of sanitizing with clean steam at > 121°C, 2.5 bar gauge), and the material surface was exposed to protein solution at periodic intervals. After the protein solution had dried, the test tank was cleaned and then analyzed for protein residues.

The test system was constructed such that it corresponded to the customary conditions in pharmaceutical production with respect to material (material grade), cleaning/sanitizing method used (time, temperature, cleaning medium, concentration of the cleaning medium) and model contamination (aqueous solution of a monoclonal antibody). Differences compared with the surfaces used in production consisted in the mechanically instead of electropolished surface of the test tank. In this connection, it must be pointed out that mechanically polished surfaces are more difficult to clean because of their larger true surface, in addition to which they accelerate rouge formation.

Table D	AES analysis of spray ball (element concentration in atom percent)						
Location	C	O	S	Ca	Cr	Fe	Ni
Surface	66	21	1	4	-	9	-
Mid Profile	-	47	-	-	-	53	-
Post Profile	6	18	-	-	11	57	8

Figure 13 SEM analysis

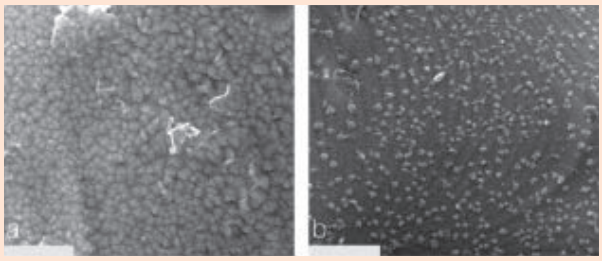

(a) bluish discolored inside surface and (b) metallic bright inside surface

Figure 14 ESCA depth profile of bluish inside surface

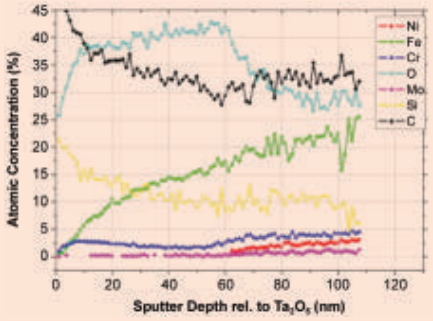

With increasing number of cleaning/sanitizing cycles, the rouging increased distinctly and the inside surface of the test tank exhibited an increasingly intensive reddish-brown color over the test duration. Four zones with rouging of different intensity and stability were formed (Figure 16).

- Zone 0: no externally applied heating jacket
- Zone 1: externally applied heating jacket
- Zone 2: externally applied heating jacket, below the liquid level, without migration rouge
- Zone 3: externally applied heating jacket, below the liquid level, with migration rouge

The formation of these different zones was explained by different heat influences of the heating jacket and by the times of exposure to the various media (sodium hydroxide solution, clean steam).

Figure 15 EDX analysis

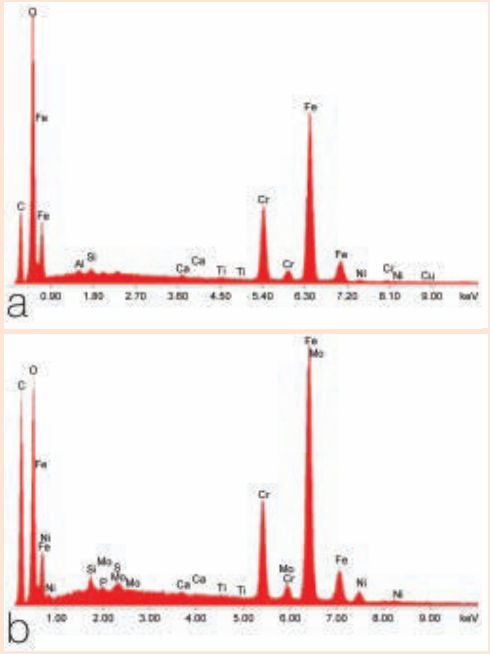

(a) tank surface sample and (b) diaphragm valve at upper tank section

Figure 16 Classification of the interior space of the test tank into zones with different rouge formation

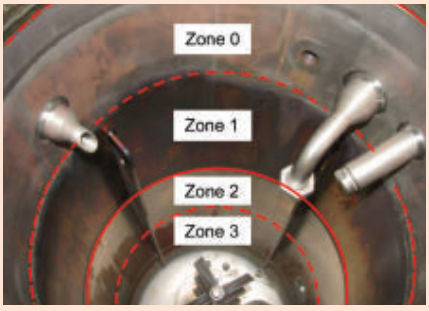

Figure 17 Results of the TOC and Swab analyses

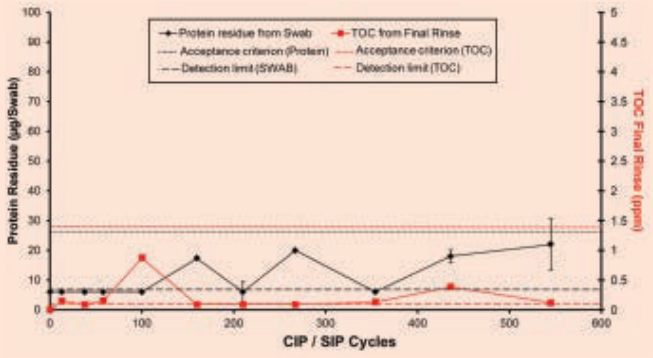

Figure 18 Test tank

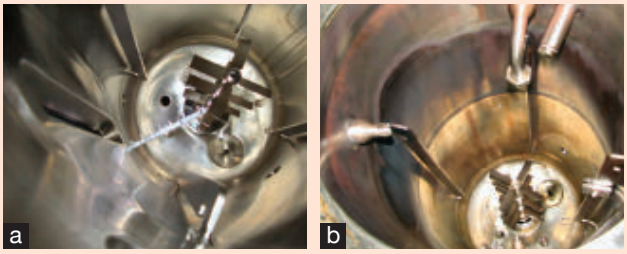

Before the beginning of the test (L) and after 545 cleaning/sanitizing cycles (R)

To measure potentially present protein residues, residue determinations were carried out using polyester fabric cloths (swabs) and TOC analyses of the post-rinse water of the cleaning process.

Even though the rouge formation increased strongly over the test period, these analyses did not reveal any trend. In all cases, the results of both analyses methods were below the specified limit values. The limit values used were derived from PI 006-3.28 Despite the very intensive rouging, no significant impairment of the cleaning efficiency was observed (Figure 17). The visual surface conditions of the test tank are illustrated in Figure 18.

Tests and practical experiences addressing further risks and influencing factors according to Table G in Part 1 will be described in Part 3 of this article.

References

1. Tverberg, J.C., Tube, T., et al., "Rouging of Stainless Steel in WFI and High Purity Water Systems," 2000.
2. Corbett, R.A., "Rouging – A Discoloration of Stainless Steel Surfaces," *Materials Performance*, Vol. 40, No. 2, Feb. 2001, p. 64-66.
3. Kane, R.D., "Rouging: The Phenomenon and Its Control in High-Purity Water Systems," *Ultrapure Water,* 23 (2006), pp. 39-43.
4. Coleman, D.C., and Evans, R.W., "Corrosion Investigation of 316L Stainless Steel Pharmaceutical WFI Systems," *Pharmaceutical Engineering*, Vol. 11, No.4, 1991, pp. 9-13, www.pharmaceuticalengineering.org.
5. Collins, S.R, and Williams, P.C., "Electropolished Tubing: Avoid Corrosion in Welded Applications – Identifying Optimum AISI 316L Composition," *Chemical Processing*, 63 (12), 2000 pp. 33-36.
6. Tuthill, A.H., Avery, R.E, and Covert, R.A., "Cleaning stainless Steel Surfaces Prior to Sanitary Service," *Dairy, Food and Environmental Sanitization*, 17 (1997), pp. 718-725.
7. R. Greene, CEP, July 2002, 15.
8. Evans, R.W., and Coleman, D.C., "Corrosion products in Pharmaceutical/ Biotech Sanitary water systems," Proceedings of Ultrapure Water EXPO´99, Philadelphia, Pennsylvania, USA, 8 April 1999.
9. Suzuki, O., Newberg, D., and Inoue, M., "Discoloration and its Prevention by Surface Treatment in High-Purity Water Systems," *Pharmaceutical Technology*, Vol. 22, No. 4, 1998, pp. 66-80.
10. Frantsen, Matheisen, Rau,Terävä, Björnstedt und Henkel: Effect of Gas Atmosphere and surface quality on Rouging of Three Stainless Steels in WFI, Force Technology.
11. Küpper, J., Egert, B., Grabke, H.J., "Entstehung und Aufbau farbiger schichten auf rostfreiem stahl: I. Verfärbungen beim Kochen von Nahrungsmitteln," *Material Corrosion*, 33 (1982) pp. 669-675.
12. Morach, R, Rouging Conference Concept, Heidelberg Feb. 2007, Rouge in pharmazeutischen Anlagen aus Sicht des Anwenders.
13. Deutsches Institut für Normung: DIN EN 10 088 Nichtrostende Stähle –Teil 1: Verzeichnis der nichtrostenden Stähle; 2011.

14. Verein Deutscher Ingenieure: VDI-Berichte; Ausgaben 235-238; 1975
15. Engineering Committee der BCI, Nichtrostender Stahl nach BN 2, 2006.
16. Gasgnier, M., and Névot, L., "Analysis and Crystallographic Structures of Chromium Thin Films," *Physica status solidi*, Vol. 66, No, 2, 1981.
17. Renner, M.,"Rouging – Werkstoffwissenschaftliche Betrachtung zu einem anspruchsvollen Phänomen," 2008.
18. Tverberg, J.C., ASM Handbook, Volume 13C, 2006.
19. International Conference on Harmonisation: ICH Q9: Quality Risk Management and local implementation in the regulatory systems of US, EU, Japan; 2005.
20. A.v. Bennekom, F. Wilke: Delta-Ferrit-Gehalt bei Werkstoff 1.4435 und der Basler Norm II; 2001
21. ISPE Baseline® *Volume 4 – Water and Steam Systems*, International Society of Pharmaceutical Engineering (ISPE), Second Edition, December 2011, www.ispe.org.
22. Hauser, G., Hygienische Produktionstechnologie, 2008.
23. Hauser, G., Hygienegerechte Apparate und Anlagen, 2008.
24. American Society of Mechanical Engineers, ASME BPE 2009, Bioprocessing Equipment, 2009.
25. European Medicines Agency, *EMEA Guideline on the Specification Limits for Residues of Metal Catalysts or Metal Reagents*, 2008.
26. Deutsches Institut für Normung: DIN 50905 Teil1-5 Durchführung von Korrosionsuntersuchungen.
27. Bee, Jared S., Chiu, David, et al., "Monoclonal Antibody Interactions with Micro- and Nanoparticles: Adsorption, Aggregation, and Accelerated Stress Studies," *Journal of Pharmaceutical Sciences*, Vol. 98, No. 9, 2009.
28. PIC/S Secretariat, *PI 006-3 PIC Recommendations on Validation Masterplan, Installation and Operational Qualification, Non-Sterile Process Validation*, Cleaning Validation, Sep. 2007, pp. 17-22.

Additional Reading

29. Henkel, B., Mathiesen, T., et al., "Using Exposure Tests to Examine Rouging of Stainless Steel, *Pharmaceutical Engineering*, Vol. 21, No. 4, July/August 2002, www.pharmaceuticalengineering.org.
30. Henkel, G. and Henkel, B., "Rouging – Hinweise zu Schichtbildungen auf Oberflächen aus austenitischen Edelstahllegierungen," *Fachbericht* Nr. 69, 2005.
31. Henkel, G., and Henkel,B., "Rougebildung auf Edelstahloberflächen 316L – Mechanismen der Bildungsreaktion," Fachbericht, Nr. 80, 2006.
32. Henkel, G., and Henkel, B., "Derouging von austenitischen Edelstahloberflächen mittels pH-neutraler Hochleistungschemikalien," *TechnoPharm*, 1 Nr. 1, 2011.
33. Henkel, G., and Henkel, B., "Derouging – or not Derouging – Ein Faktenabgleich," *Pharmind*, 73 Nr. 9, 2011.

Table E ESCA analysis of spray ball (element concentration in atom percent)

Location	Na	Zn	Fe	O	N	Ca	C	Cl	S	Si	P
Degrease and Sputtered Surface	0.5	-	30.1	46.3	3.3	0.6	17.2	0.2	0.2	1.6	-

Table F Results of optical inspection and SEM analysis of wipe samples

Components	Optical Appearance	SEM Analysis of Wipe Samples
Buffer tank	Reddish discoloration, particularly above the lower weld seam Upper tray showing slight multi-colour discoloration	Especially oxygen, iron and chromium were determined in the coatings. Trace amounts of nickel and molybdenum were also present
Lower connection piece	Slight reddish discoloration	Small oxygen content; composition of the alloying elements iron, chromium nickel and molybdenum conform to the alloy content of the material of construction
Diaphragm valve at upper tank section	Slight reddish discoloration	A greater oxygen content again shows a defined iron and chromium peak and diminishing nickel and molybdenum contents

Table G Corrosion rate of standard austenitic stainless steels, 108°C, 21 days

Material No.	Number of Samples	Corrosion Rate (mm/a)	Appearance
1.4301	1	0.0018	Metallic bright
1.4571	1	0.0004	Metallic bright
1.4404	4	0.0004 - 0.0014	Metallic bright
1.4435	1	0.0010	Metallic bright

Table H Heavy metal concentrations in various water circuits, determination by means of ICP MS

Unit	Fe (ppm)	Cr (ppm)	Ni (ppm)	Mo (ppm)
Unit 1: Deionized water	1.8	< 0.1	< 0.1	< 0.1
Unit 1: WFI hot normal operation	< 1.0	0.13	0.16	< 0.1
Unit 1: WFI cold	< 1.0	< 0.1	0.18	< 0.1
Unit 1: WFI after 12 days without water withdrawal	< 1.0	< 0.1	< 1.0	< 0.1
Unit 2: WFI normal operation	< 1.0	< 0.1	< 1.0	< 0.1
Unit 2: WFI after two month without water withdrawal	< 1.0	< 0.1	6.6	< 0.1
Limit of Quantitation (ICP-MS)	1.0	0.1	0.1	0.1
Limit value (EMEA Guideline)	130	2.5	2.5	2.5

Table I Heavy metal concentrations of various active pharmaceutical ingredients from different production systems.

Production System	API (Active Substance)	Plant placed in service (year)	Derouging (year)	Fe (ppm)	Mn (ppm)	Ni (ppm)	Cr (ppm)	Mo (ppm)
System 1	API 1	1998	2008	< 0.6	< 0.06	< 0.09	< 0.06	< 0.02
System 2	API 1	2006	n/a	< 0.6	< 0.06	< 0.09	< 0.06	< 0.02
System 2	API 2	2006	n/a	< 0.6	< 0.06	< 0.09	< 0.06	< 0.02
System 3	API 3	2003	n/a	< 0.6	< 0.06	< 0.09	< 0.06	< 0.02
System 4	API 3	2005	n/a	< 0.6	< 0.06	< 0.09	< 0.06	< 0.02
System 5	API 4	2004	2008	< 0.6	< 0.06	< 0.09	< 0.06	< 0.02
System 5	API 5	2002	2008	< 0.6	< 0.06	< 0.09	< 0.06	< 0.02
Limit of Quantitation (ICP-MS)				0.6	0.06	0.09	0.06	0.02
Limit (EMEA Guideline)				130	25	2.5	2.5	2.5

Date of the retention samples of the investigated products: May to December 2010; analyses were performed from November 2010 to March 2011

34. Zeiff, A. and Homburg, D., et al., "Umweltschonendes Derougen von Edelstahloberflächen," *Process*, 2008.
35. Vernier, M., "Wenn Edelstahl errötet," CITplus, Nr. 5, 2007.
36. Czech, A., "Rouging – Erfahrungen aus der Praxis am Beispiel einer WFI-Anlage," *Pharmind*, 73 Nr. 1; 2011.

About the Authors

Thomas Blitz studied chemical engineering at the University of Darmstadt and holds a Dipl. Ing.

Ernst Felber was educated as a technical glass blower, AVOR and draughtsman and received further education in material engineering.

Robert Haas (Dipl. Ing. (FH)) graduated with a degree in bioengineering at the University of Applied Sciences in Munich.

Birgit Lorsbach studied materials engineering at the University of Applied Science in Aalen and graduated as an engineer (FH).

Andreas Marjoram studied chemical engineering at the University of Applied Science in Berlin completing studies in chemical engineer (biological process) and industrial engineering (same university, 2006-2010) where he completed an MSc in industrial engineering.

Roland Merkofer studied mechanical engineering FH and business administration FH.

Tobias Müller is with Roche Diagnostics GmbH, Penzberg, Germany. He graduated as a master craftsman in chemistry in 1998.

Dr. Nathalie Schuleit graduated in material science at engineering school from the University of Paris and received her PhD from the École des Mines de Saint Etienne, France in the area of hard thin coatings for forming tools.

Marc Vernier studied chemical engineering at the University of Applied Sciences of Muttenz (Switzerland), with additional education in business administration.

Dr. Thomas Wellauer, PhD, received his PhD in Chemistry from the University of Basel.